Recovery of partially occluded objects by applying compressive Fresnel holography

Yair Rivenson,[1,*] Alon Rot,[1] Sergey Balber,[1] Adrian Stern,[2] and Joseph Rosen[1]

[1]*Department of Electrical and Computer Engineering, Ben-Gurion University of the Negev, P.O. Box 653, Beer-Sheva 84105, Israel*

[2]*Department of Electro-Optics Engineering, Ben-Gurion University of the Negev, P.O. Box 653, Beer-Sheva 84105, Israel*

**Corresponding author: rivenson@ee.bgu.ac.il*

Received January 9, 2012; revised March 1, 2012; accepted March 1, 2012;
posted March 2, 2012 (Doc. ID 161160); published May 15, 2012

A compressive Fresnel holography approach is suggested for the recovery of partially occluded objects. Reconstruction guarantees are analyzed and the effectiveness of the method is demonstrated using simulations and an experimental result showing the reconstruction of a partially occluded resolution chart.

OCIS codes: 090.1995, 070.0070, 100.3190, 110.1758.

The reconstruction of partially occluded objects has been a subject of research in recent years. Generally, one wishes to see through a partially occluding plane in order to get a clear image of a specific target object. In the last decades, advancements in digital image sensors and computation capabilities have yielded several opportunities to tackle this problem, where most techniques involve the sensing of the scene from different directions [1–4]. By proper synthesis of the captured perspectives, the object is recovered. Synthesizing different object perspectives to reconstruct an object was also adapted to holography [5]. However, each perspective has degraded resolution compared with the original hologram, which may impair the overall performance of the method.

In this letter we offer a general technique to recover a partially occluded object from its digitally recorded single hologram using the compressive sensing (CS) approach. CS has already gained ground in the realm of holography [6–10]. The CS approach asserts that given the fact that a signal is sparse, or compressible in some (known) transform domain, $\boldsymbol{\Psi}$, it can be fully recovered by taking only a subset of its measurements, using some sensing operator, which should hold low coherence with the sparsifying operator. Figure 1 depicts our basic setup: a coherently illuminated object field, u_{in}, with wavelength λ, propagates a distance z_1 and hits a partially occluding plane made of opaque and clear or scattering regions, and is given by $p(x)$. This may be regarded as a subsampling of the object's Fresnel field; hence the motivation of using the compressive Fresnel holography approach. The wavefield than propagates another distance z_2 and interferes with a reference wave on a CCD. The object's field, $u_{\text{ccd}}(x)$, can be extracted using standard techniques, such as filtering out the unwanted diffraction terms [11], and is described by

$$u_{\text{ccd}}(x) = \left\{ u_{\text{in}} * \frac{\exp[j\pi x^2/(\lambda z_1)]}{\sqrt{\lambda z_1}} p(x) \right\} * \frac{\exp[j\pi x^2/(\lambda z_2)]}{\sqrt{\lambda z_2}}. \tag{1}$$

For simplicity, we derive our equations for a one-dimensional (1D) system. Equation (1) is often described in CS literature as a vector-matrix multiplication form:

$$\mathbf{u}_{\text{ccd}} = \boldsymbol{\Phi}\mathbf{u}_{\text{in}}, \tag{2}$$

where $\boldsymbol{\Phi}$ denotes the sensing matrix.

In [9] we have determined reconstruction guarantees when the Fresnel transform is used as a compressive sensing mechanism, where the hologram plane is subsampled. Therefore, it can be viewed as the scheme in Fig. 1, with $z_2 = 0$ and $p(x)$ binary with its 1s and 0s assigned *uniformly at random*. Here, we consider realistic general occluding planes; thus, we allow $p(x)$ to receive any value between 0 and 1 and also allow deterministic structures as well. Often, CS literature deals with nonrandom subsampling schemes by analyzing the sensing matrix columns coherence [12], given by

$$\mu = \mu(\boldsymbol{\Phi}) = \max_{m \neq l} |\langle \phi_m, \phi_l^* \rangle| / \{ \|\phi_m\|_2 \|\phi_l\|_2 \}, \tag{3}$$

where ϕ_l denotes the lth column vector of $\boldsymbol{\Phi}$. The smaller μ is, the fewer samples are needed in order to accurately reconstruct the signal [12]. We note that the second propagation along z_2 can be expressed as a unitary transform, which does not subsample the signal and has no effect on the coherence of the sensing system (though it may have a preconditioning effect on the system [13]). Therefore, we may analyze the coherence of the sensing operator from two subsampled fields originated from two different source points, m and l, and hitting the occluding plane as follows:

$$\mu = \max_{m \neq l} |\langle \tilde{\phi}_m, \tilde{\phi}_l^* \rangle| / \{ \|\tilde{\phi}_m\|_2 \|\tilde{\phi}_l\|_2 \}, \tag{4}$$

where

$$\tilde{\phi}_l = \delta(x - l) * \exp[j\pi x^2/(\lambda z_1)] / \sqrt{\lambda z_1} p(x). \tag{5}$$

In digital holography the signal is reconstructed using numerical backpropagation, which is normally carried

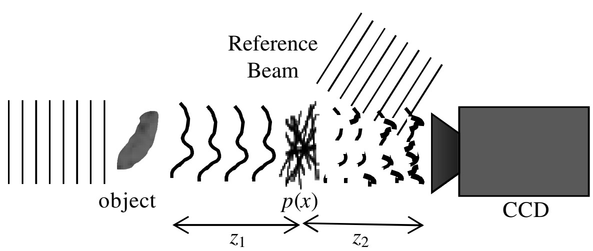

Fig. 1. (Color online) A schematic setup for a partially occluded object's wavefield acquisition.

0146-9592/12/101757-03$15.00/0

out by the far-field (direct method) numerical approximation or near-field (convolution method) numerical approximation [11,14]. Following the approach in [9], defining Δx_o as the object's pixel pitch, Δx_{z1} as the occluding plane pixel pitch, and N as the number of pixels, the far-field numerical approximation is given by

$$\begin{aligned}\tilde{\phi}_l(q\Delta x_{z1}) &= \frac{1}{\sqrt{\lambda z_1}} p(q\Delta x_{z1}) e^{\frac{j\pi}{\lambda z_1}(l\Delta x_o - q\Delta x_{z1})^2} \\ &= \frac{1}{\sqrt{\lambda z_1}} p(q\Delta x_{z1}) e^{\frac{j\pi}{\lambda z_1}(l\Delta x_o)^2} e^{\frac{j\pi}{\lambda z_1}(q\Delta x_{z1})^2} e^{-\frac{j2\pi}{\lambda z_1} lq\Delta x_o \Delta x_{z1}},\end{aligned} \tag{6}$$

where $0 \le l \le N-1$. Substituting Eq. (6) in Eq. (4) we find that μ for the far-field numerical approximation is given by

$$\begin{aligned}\mu_{\mathrm{FF}} &= \max_{m\neq l} \frac{\frac{1}{\lambda z_1}\left|\sum_{q=1}^{N}\left|p(q\Delta x_{z1})\right|^2 e^{-j\frac{2\pi}{\lambda z_1}\Delta x_o \Delta x_{z1} q(m-l)}\right|}{\sqrt{\frac{1}{\lambda^2 z_1^2}\sum_{q=1}^{N}\left|p(q\Delta x_{z1})\right|^2 \sum_{q=1}^{N}\left|p(q\Delta x_{z1})\right|^2}} \\ &= \max_{m\neq l}\left|\widehat{\mathrm{P}}\left(\frac{m-l}{\lambda z_1}\Delta x_o \Delta x_{z1}\right) \right. \\ &\qquad \left. \otimes\, \widehat{\mathrm{P}}\left(\frac{m-l}{\lambda z_1}\Delta x_o \Delta x_{z1}\right)\right| \Big/ \sum_{q=1}^{N}\left|p(q\Delta x_{z1})\right|^2.\end{aligned} \tag{7}$$

where $\widehat{\mathrm{P}} = \mathbf{F}\{p\}$, $\mathbf{F}$ is the discrete Fourier transform, $\otimes$ is the correlation operator, and FF stands for far field.

As for the near-field numerical approximation where the diffraction is small and $\Delta x_o = \Delta x_{z1}$, we obtain from [14]:

$$\begin{aligned}\tilde{\phi}_l &= p(q\Delta x_o)\mathbf{F}^{-1}\{\exp\{-j\pi\lambda z_1(n\Delta v)^2\}\mathbf{F}\{\delta[(s-l)\Delta x_o]\}\} \\ &\approx e^{-j\frac{\pi}{4}}\frac{\Delta x_o}{\sqrt{\lambda z_1}} p(q\Delta x_o) e^{\frac{j\pi}{\lambda z_1}\Delta x_o^2 (q-l)^2}\,\mathrm{rect}\left[\frac{(q-l)N\Delta x_o^2}{\lambda z_1(N-1)}\right],\end{aligned} \tag{8}$$

where $n, s = 0, 1, 2, \ldots N-1$ and $\Delta v = 1/(N\Delta x_o)$. By substituting Eq. (8) into Eq. (4) we get

$$\begin{aligned}\mu_{\mathrm{NF}} &\approx \max_{m\neq l}\left|\frac{\Delta x_o^2}{\lambda z_1}\sum_{q=1}^{N}|p(q\Delta x_o)|^2 \mathrm{rect}\left[\frac{(q-l)N\Delta x_o^2}{(N-1)\lambda z_1}\right]\right. \\ &\qquad \left.\times\,\mathrm{rect}\left[\frac{(q-m)N\Delta x_o^2}{(N-1)\lambda z_1}\right] e^{-j2\pi\frac{\Delta x_o^2}{\lambda z_1}q(m-l)}\right| \Big/ \|\tilde{\phi}_m\|_2 \|\phi_l\|_2.\end{aligned} \tag{9}$$

The result of Eq. (9) depends on the object's Fresnel number, which dictates the width of the two rect{} functions and the structure of the occluding plane, p. In general, an analytical result cannot be obtained, and each case should be considered separately. However, in the case that the occluding plane is composed from binary entries generated uniformly at random, we have shown in [9] that $\mu_{\mathrm{FF}} \le \mu_{\mathrm{NF}}$. Empirically, we have witnessed that $\mu_{\mathrm{FF}} \le \mu_{\mathrm{NF}}$ in numerous numerical experiments we have performed.

In order to demonstrate the dependence of μ on the occluding structure, we have created two 128×128 random binary masks, where 80% of the pixels are opaque. The first subsampling mask was composed from 2×2 opaque patches [Fig. 2(a)], where the second was composed from 8×8 opaque patches [Fig. 2(c)]. From Figs. 2(b) and 2(d) we witness that μ_{FF} increases as the size of the patches increase. This was also verified with a numerical simulation with different occluding planes and subsampling ratios, with the results shown in Fig. 3. The occluding planes were composed from different sizes of opaque squares (1×1, 8×8, 16×16, and 32×32 pixels). The object was the 256×256 Lena image, and we have chosen parameters such that the numerical far-field approximation model is valid. After simulating both field propagations, signal reconstruction is obtained by solving the following problem:

$$\min \|\boldsymbol{\Psi}\mathbf{u}_{\mathrm{in}}\|_1 + \alpha \mathrm{TV}(\mathbf{u}_{\mathrm{in}}) \quad \text{s.t. } \|\mathbf{u}_{\mathrm{out}} - \boldsymbol{\Phi}\mathbf{u}_{\mathrm{in}}\|_2 < \varepsilon, \tag{10}$$

where TV is the total variation functional [6–9,12]. We set the estimated noise level with ε; $\boldsymbol{\Psi}$ is the sparsifying operator, which in our case was the Haar wavelet transform; and α is a regularization parameter. In order to solve the problem formulated in Eq. (10) we have used the SolveTV solver [12,15]. A successful image reconstruction threshold was set to 30 dB PSNR. From Fig. 3 it is evident that the reconstruction success drops as the occluding plane is getting more structured and μ increases.

We have also validated the applicability of the method by an experiment. An Edmund Optics 1951 U.S. Air Force (USAF) transmission resolution chart was illuminated using a collimated HeNe laser beam with wavelength of 632 nm. As a partially occluding object we have used a twisted, blackened barbed wire. The distance between the object and occluding plane was approximately 10 cm. An $f = 250$ mm lens was used in order to increase the field of view. It was set 12 cm away from the occluding barbed wire and 40 cm from an Allied Vision Tech. Manta

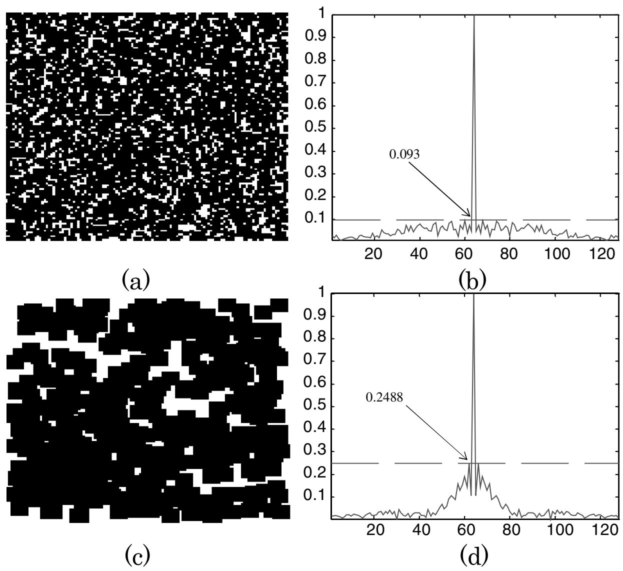

Fig. 2. (Color online) (a), (c) Partially occluding planes. (b), (d) Corresponding cross sections of $|\langle\phi_m, \phi_l^*\rangle|/\{\|\phi_m\|_2\|\phi_l\|_2\}$, of (a) and (c), respectively. μ_{FF} is marked with a dotted line.

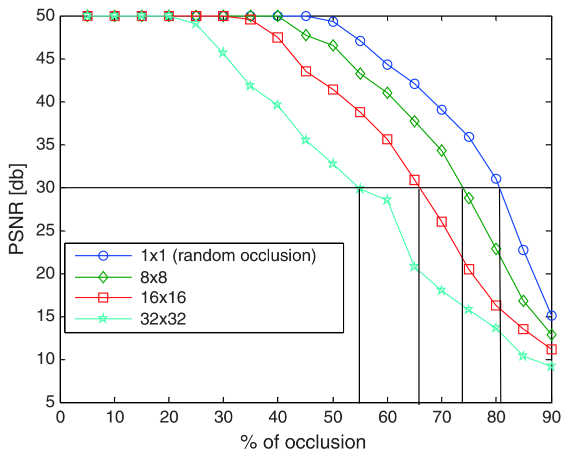

Fig. 3. (Color online) Reconstruction PSNR as a function of occluding percentage for occluding planes with different square sizes, which yield different μ_{FF}.

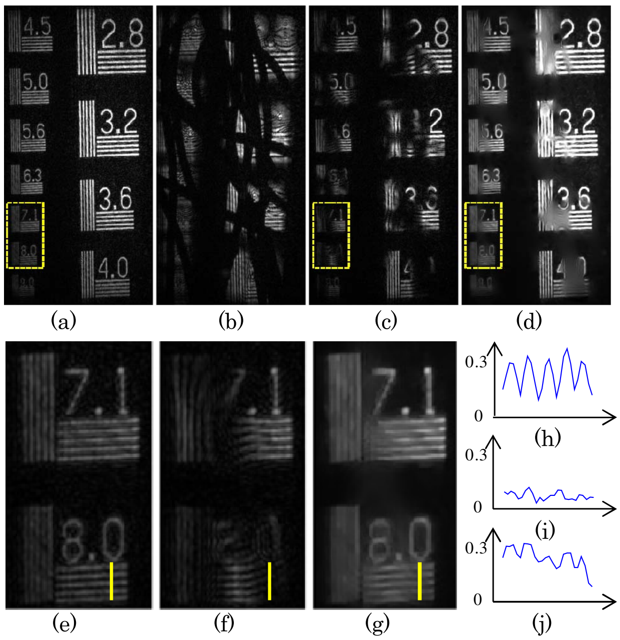

Fig. 4. (Color online) (a) Reconstruction of the USAF chart without the occluding plane, using standard Fresnel backpropagation, for reference. (b) Focusing on the occluding plane, from which the occluding function was extracted from. (c) Same as (a), but this time the occluding plane distorts the reconstructed object plane. (d) Same experiment as (c), but applying the CS framework to reconstruct the object plane. (e), (f), and (g) zoom in on the highlighted parts of (a), (c), and (d) respectively. (h), (i), and (j) correspond to the highlighted cross sections of (e)–(g).

G-145 CCD camera with 1390 × 1038 pixels and pixel size of 6.45 μm. This setup yields a reconstruction distance of $z_1 \approx 4$ cm, which corresponds to a numerical near-field approximation regime [9]. An off-axis holography setup was used with a slightly tilted reference wave. Prior to the reconstruction stage the unwanted orders were filtered out. By focusing on the occluding plane, p, we have found $\mu_{NF} \approx 0.175$, where approximately 59% of the object field is obscured by the occluding plane. Generally, a joint estimation of both signal and system is a nontrivial problem requiring a priori information. In our case we assumed that the occluding plane, p, can be modeled as a binary function (because we expect no light has passed through the wires) with completely unknown spatial distribution. This a priori knowledge enabled the estimation of the occluding plane using a thresholding procedure.

Figures 4(a) through 4(j) show the reconstruction results. It is evident that the reconstruction with the suggested CS-based approach reveals details that are lost in the reconstruction with numerical backpropagation.

In conclusion, we have analytically derived reconstruction bounds for a partially occluded Fresnel field when applying the CS framework. These results are a generalization of previous results [9]. We then demonstrated by simulations and an experiment the effectiveness of using the CS framework for the reconstruction of partially occluded objects from their hologram recording. The object reconstruction is owed to the holographic acquisition process, which allows the sensing of the object's partially occluded field using a single shot. This would otherwise be impossible with a respective incoherent imaging system, which uses a single shot and a single aperture. Further future works can generalize the concept to 3D obstacles or compensate for the occluding plane's measurement uncertainties, which is essential for successful reconstruction.

This research was partially supported by the Israel Science Foundation (grant No. 1039/09) and Israel's Ministry of Science and Technology.

References

1. B. Javidi, R. Ponce-Díaz, and S.-H. Hong, Opt. Lett. **31**, 1106 (2006).
2. Y. S. Hwang, S.-H. Hong, and B. Javidi, J. Display Tech. **3**, 64 (2007).
3. N. Joshi, S. Avidan, W. Matusik, and D. J. Kriegman, in *IEEE 11th International Conference on Computer Vision* (2007).
4. M. Levoy, B. Chen, V. Vaish, M. Horowitz, I. McDowall, and M. Bolas, ACM Trans. Graphics **23**, 825 (2004).
5. J. Maycock, C. P. McElhinney, B. M. Hennelly, T. J. Naughton, J. B. McDonald, and B. Javidi, Appl. Opt. **45**, 2975 (2006).
6. Y. Rivenson, A. Stern, and B. Javidi, J. Display Tech. **6**, 506 (2010).
7. M. M. Marim, M. Atlan, E. Angelini, and J.-C. Olivo-Marin, Opt. Lett. **35**, 871 (2010).
8. Y. Rivenson, A. Stern, and J. Rosen, Opt. Express **19**, 6109 (2011).
9. Y. Rivenson and A. Stern, Opt. Lett. **36**, 3365 (2011).
10. S. Lim, D. L. Marks, and D. J. Brady, Appl. Opt. **50**, H75 (2011).
11. T. Kreis, *Handbook of Holographic Interferometry*, 1st ed. (Wiley-VCH, 2004), Chap. 3.
12. M. Lustig, D. L. Donoho, and J. M. Pauly, Magn. Reson. Med. **58**, 1182 (2007).
13. A. Bourquard, F. Aguet, and M. Unser, Opt. Express **18**, 4876 (2010).
14. L. Yaroslavsky, in *Advances in Signal Transforms: Theory and Applications*, J. Astola and L. Yaroslavsky, eds., EURASIP Book Series on Signal Processing and Communication (2007).
15. Available at http://www.cs.ubc.ca/labs/scl/sparco.